

# Evaluation of a Novel Method of Real time Computer Assisted Spine Surgery

Nobert Thomas Pallath\*, Tessamma Thomas\*, S. Suresh\*\*

\* Department of Electronics, Cochin University of Science & Technology

\*\* Department of Orthopaedics, Lakeshore Hospital & Research Centre

**Abstract-** In this paper the effectiveness of a novel method of computer assisted pedicle screw insertion was studied using testing of hypothesis procedure with a sample size of 48. Pattern recognition based on geometric features of markers on the drill has been performed on real time optical video obtained from orthogonally placed CCD cameras. The study reveals the exactness of the calculated position of the drill using navigation based on CT image of the vertebra and real time optical video of the drill. The significance value is 0.424 at 95% confidence level which indicates good precision with a standard mean error of only 0.00724. The virtual vision method is less hazardous to both patient and the surgeon.

**Index Terms-** computer assisted spine surgery (CASS); pedicle screw; micro-motor drill; pattern matching; graphical overlay

## I. INTRODUCTION

The basic principle in surgery is to restrict the iatrogenic trauma done to a patient to a minimum. Modern surgical technology and technique have shifted this principle into a new dimension. However, the surgical strategy depends on the localization and patho-anatomy of the region or structure which has to be treated (Fig.1).

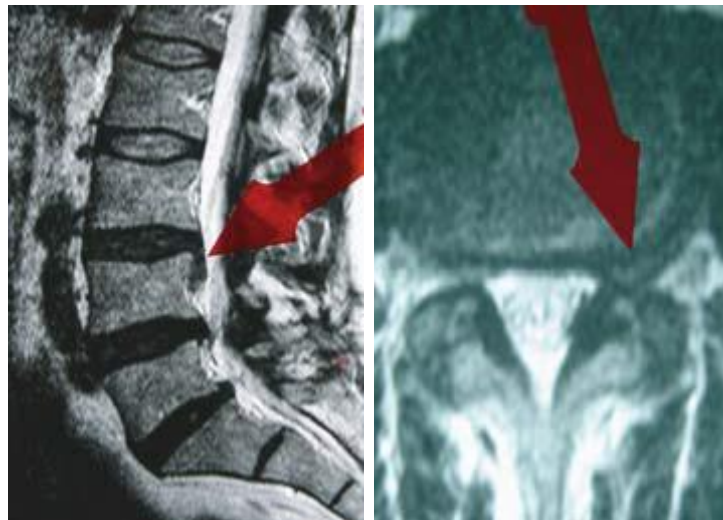


**Figure.1 Different localization, size, and configuration of surgical targets**

Topography and volumetry of the target must be clear. This information is usually given by different imaging techniques such as MRI, CT, etc. [1]. One of the major advantages lies in the possibility to perform operations through small skin incisions (“keyhole surgery”). This needs meticulous preoperative planning, exact positioning of the patient, and reliable localization of the surgical target area in projection to the entry level on the skin surface, there are some objections which might depend on the surgical training, the acquired surgical philosophy, as well as the age and experience of the individual surgeon[2][3]. This is one of the difficulties which are faced by the surgeon at the beginning of his individual learning curve. Quite often removal of bone becomes necessary [4][5]. Important tools used to enter the spinal canal and to enlarge the spinal canal are high-speed drills which perform quick and precise dissection of bone

structures. High-speed drills guarantee flat smooth surfaces without edges and spurs [6][7][8].

With the advent of precise pre and intra operative imaging means, the development of sophisticated image data visualization, and the accessibility of sub milli metric, real-time tracking of objects in space, surgical navigation systems have been created that aim at enhanced surgical accuracy and ultimately improved clinical outcome [9][10][11][12][13][14]. Numerous studies have shown the superiority of computer-assisted versus conventional instrumentation at different levels of the spine regarding accuracy and thus potential safety [15][16][17][18][19][20][21]. Although pre-operative CT-imaging or registration is not required in fluoroscopy based navigation systems, CT based navigation systems have definite advantage with respect to precise preoperative planning using 3D

visualization of patient anatomy [22]. Moreover, x-ray fluoroscopic technique has definite side effects, due to considerable radiation exposure to the patient and the surgical staff [23]. Also, it cannot be used during the entire screw insertion procedure due to possible spatial conflicts between C-frame, the surgeon and the surgical instruments [24]. Surgical robots are voluminous and occupy too much of the operating room space [24][25]. Registration and immobilization are two key issues in robot assisted surgery [26]. Also, commercial surgical robots are extremely costly. Although these methods claim over 90 percent accuracy, their use is limited to few large research hospitals [24][27]. In this paper, we present the evaluation of a novel method of computer assisted surgery, with low instrumentation cost and high precision using real time video processing and computer graphics.

## II. METHODS AND MATERIALS

The method developed is based on real time processing of the video grabbed using the experimental setup, consisting of cadaveric dry human vertebra, phantom model of the vertebra, micro motor drill, Cohu DSP

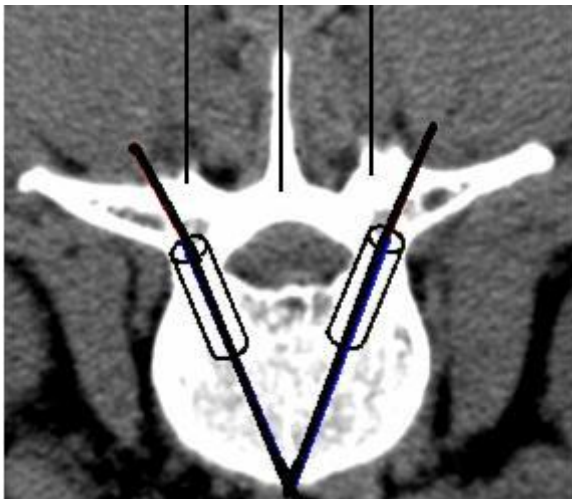


**Figure.2 An example of the reference image**

3600 cameras, workstation computer with matrox morphis frame grabber, in a created surgical environment. The optimum distance, position, yaw, pitch and roll of the camera are fixed. The camera is placed in a position considering the entire surgical setup, like patient position, lighting and also without causing any obstruction to the surgeon and the entire surgical set up. The workstation computer is arranged with the monitor at a viewable distance.

### A. Pre-operative Planning

Pre-operative planning is an important step in the procedure which involves the analysis and measurement of the pedicle parameters viz., width, height and orientation. The preoperative axial CT- image of the spine is used for this purpose. The step involves identification of the vertebrae where the pedicle screw is to be inserted, selection of the appropriate representative image of the vertebra, marking the landmark points on the selected

image and computing the parameters of the pedicle like width and height. The process is done for both the vertebrae used for fusing. 3D doctor software is used for vertebra modelling and measurements [24]. A one inch square marker with a unique geometric shape is designed by considering the shapes of all background objects so as to avoid ambiguity and false detection during object search. The marker is fixed centrally on the body of the micro motor drill. An alternate method of fixing the marker on the drill owl is also used for tracking the pedicle screw. The axis of the drill or drill owl passes through the centroid of the marker. The axial CT image of the candidate vertebra consists of eight or nine slices at a separation of 2 to 3 mm. The fourth or fifth slice is the best representative image [24]. This image provides a clear picture about the pedicle dimensions, from normal anatomy. The image as shown in the figure1 is used to determine the pedicle width, angle and relationship with other anatomical structures. A vertical line is drawn through the middle of the transverse process and equidistant lines from the central lines drawn in each of the spinous process as shown in figure 2, aid in the registration step [24]. Registration of the CT image and the actual vertebra is done by overlaying. Two lines drawn through the centre of the pedicle area from the lamina to the vertebra body as shown in figure1, displays the ideal reference path for pedicle screw insertion [24]. The anatomy of the pedicle shows that, it has a non-uniform cylindrical shape, with varying diameter across its length [24]. Graphical cylinder plotted with diameter, fixed using minimum width of the pedicle area as shown in figure1, aids in visualization of the trajectory and tracking of the pedicle screw during insertion [24].

### B. Camera Calibration

Relationship between pixel coordinates and real world coordinates is established using camera calibration. A dot pattern grid is used to map pixel coordinates to real world coordinates, for accurate analysis and measurement of the drill position and orientation. A square grid pattern is used, for detecting perspective distortions due to camera lens. The mapping physically corrects image distortions, viz. non unity aspect ratio distortion, rotation distortion, perspective distortion, pincushion distortion and barrel type distortion. The results are returned in real world units, which automatically compensates for any distortions in the image. A calibration object is used to hold the defined mapping and used to transform pixel coordinates or results to their real world equivalents.

Using the theorem of intersecting lines [28], the computational model of the pinhole camera model is denoted by:

$$\begin{pmatrix} u \\ v \end{pmatrix} = \frac{f}{z} \begin{pmatrix} x \\ y \end{pmatrix} \quad [28]$$

where, x, y, z the coordinates of a scene point in the 3D coordinate system whose origin is the projection center and u, v denote the image coordinates. The parameter f is known as the camera constant; it denotes the distance from the projection center to the image plane.

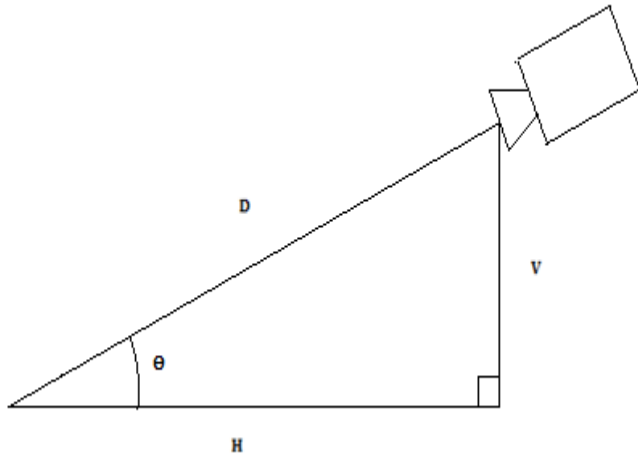


**Figure 3. Camera placement and distances**

From figure 3,

$$\begin{pmatrix} u \\ v \end{pmatrix} = \frac{f}{D} \begin{pmatrix} x \\ y \end{pmatrix} \quad (1)$$

Where  $z \approx D$  the axial distance.

Also

$$D = \sqrt{V^2 + H^2}$$

$$u = \frac{f}{\sqrt{V^2 + H^2}} \times x \quad (2)$$

From equation (2),

$$(u_1 - u_2) = \frac{f}{\sqrt{V^2 + H^2}} \times (x_1 - x_2)$$

Therefore,

$$\frac{(u_1 - u_2)}{(x_1 - x_2)} = \frac{f}{\sqrt{V^2 + H^2}}$$

Let  $P_d$  be the Pixel distance with respect to the object displacement  $R_d$ . Therefore, the Euclidean distance between any two pixel positions is,

$$P_d = P_{d1} - P_{d2} = \sqrt{(u_1 - u_2)^2 + (v_1 - v_2)^2}$$

The corresponding object displacement,

$$R_d = R_{d1} - R_{d2} = \sqrt{(x_1 - x_2)^2 + (y_1 - y_2)^2}$$

The ratio,

$$\frac{P_d}{R_d} = \frac{\sqrt{(u_1 - u_2)^2 + (v_1 - v_2)^2}}{\sqrt{(x_1 - x_2)^2 + (y_1 - y_2)^2}} \quad (3)$$

From equation (2),

$$\frac{\sqrt{(u_1 - u_2)^2 + (v_1 - v_2)^2}}{\sqrt{(x_1 - x_2)^2 + (y_1 - y_2)^2}} = \frac{f}{\sqrt{V^2 + H^2}}$$

Therefore,

$$\frac{P_d}{R_d} = \frac{f}{\sqrt{V^2 + H^2}} \quad (4)$$

Or,

$$f = \frac{P_d}{R_d} \times \sqrt{V^2 + H^2} \quad (5)$$

Using a set of object points  $\{ (x_1, y_1), (x_2, y_2), \dots, (x_n, y_n) \}$ , the corresponding image points  $\{ (u_1, v_1), (u_2, v_2), \dots, (u_n, v_n) \}$ , are obtained using the camera and the ratio " $P_d/R_d$ " is found out from (3). Next, the value of  $V$  and  $H$  are measured after fixing the camera. Knowing the ratio " $P_d/R_d$ ",  $V$  and  $H$ , the value of  $f$  is found out using (5). Now, knowing,  $V$  and  $H$ , the value of " $R_d$ " can be found out for every measured " $P_d$ ".

### C. Registration and Surgery

After surgical exposure of the spine, one needle is placed in the middle of the superior articular process and two needles are placed, on the spinous process, at distances measured during the pre-operative planning phase [24]. By overlaying the transparent reference image, with lines drawn as mentioned in section [II A], over the video and adjusting the focus and zoom of the camera, the three needles in the video, are exactly made to coincide with the three vertical lines, plotted on the reference image. At this stage, the dimensions of the objects in both the images match, which finalizes the registration process. Now, the drill is positioned with its burr exactly placed at the entry point. Using computer graphics, the cylinder and its axis, with the required height and diameter, measured during the pre-planning phase, are created.

Square marker with 2.5 cm x 2.5 cm dimension, having a unique geometric shape is designed by considering the shapes of all background objects, so as to avoid ambiguity and false detection. Marker is fixed centrally on the body of the micro motor drill, so as to face the camera. An alternate method is to fix the marker, on the drill owl, so as to track the pedicle screw. The axis of the drill or drill owl passes through the centroid of the marker. The video of the drill, with the marker fixed centrally on its body is grabbed and processed in sequential frames.

The procedure begins by correcting the orientation of the drill so that, it correctly enters the pedicle canal and the vertebral body. The orientation of the drill is same as the marker orientation. Now, the path of the drill is tracked during insertion, to ensure that it does not go beyond the walls of the pedicle canal or pierce the vertebra body. The method is to search the marker, using edge extraction to get the geometric features of the marker. The search is performed and results are displayed, based on calibration. The algorithm uses edge based geometric features of the models and the target, to establish match. Gradient method is

used, for extracting object contours. An object contour is a type of edge that defines the outline of the objects in an image. The edges extracted from the video frame are used to form the image's edge map, which represents how the image is defined as a set of edges. The feature calculations are performed using the image's edge map. The edge finding method uses operations that are based on differential analysis, where edges are extracted by analyzing intensity transitions in images. Edges are extracted in three basic steps. First, a filtering process provides an enhanced image of the edges, based on the computations of the image's derivatives. Second, detection and thresholding operations determine all pertinent edge elements, or edgels from the image. Third, neighboring edgels are connected to build the edge chains and features are calculated for each edge. The enhanced image of the object contours is obtained by calculating gradient magnitude of each pixel in the image.

First order derivatives of a digital image are based on various approximations of the 2D gradient. The gradient of an image  $f(x, y)$  at the location  $(x, y)$  is defined as the vector [29]:

$$\nabla f = \begin{pmatrix} G_x \\ G_y \end{pmatrix} = \begin{pmatrix} \frac{\partial f}{\partial x} \\ \frac{\partial f}{\partial y} \end{pmatrix} \quad (6)$$

The gradient magnitude is calculated at each pixel position, from the image's first derivatives. It is defined as [29]:

$$= \text{mag}(\nabla f) = \sqrt{G_x^2 + G_y^2} \quad (7)$$

An edgel or edge element is located at the maximum value of the gradient magnitude over adjacent pixels, in the direction defined by the gradient vector. The gradient direction is the direction of the steepest ascent at an edgel in the image, while the gradient magnitude is the steepness of that ascent. Also, the gradient direction is the perpendicular to the object contour. The marker with the unique geometric shape is fixed as the search model. The search of instances of models in the sequence of video frames is performed. The match between the model and its occurrences in the target image is determined using the values of "score" and "target score". The score is a measure of active edges of the model found in the occurrence, weighted by the deviation in position of these common edges. The model scores are calculated as follows.

Score = Model coverage  $\times$  (1- (Fit error weighing factor  $\times$  Normalized Fit Error))

Target score = Target coverage  $\times$  (1- (Fit error weighing factor  $\times$  Normalized Fit Error))

The model coverage is the percentage of the total length of the model's active edges, found in the target image. 100% indicates that, for each of the model's active edges, a corresponding edge was found in the occurrence. The target coverage is the percentage of the total length of the model's active edges, found in the occurrence, divided by the length of edges present within the occurrence's bounding box. Thus, a target coverage score of 100 % means that, no extra edges were found. Lower scores indicate that, features or edges found in the target are not present in the model. The fit error is a measure of how well the edges in the occurrence, correspond to those of the model. The fit error is calculated as the average quadratic

distance, in pixels or calibrated units, between the edgels in the occurrence and the corresponding active edges in the model.

$$\text{Fit error} = \frac{\sum_{\text{all common pixels}} [(\text{error in } x)^2 + (\text{error in } y)^2]}{\text{Number of common pixels}}$$

A perfect fit gives a fit error of 0.0. The fit error weighing factor (between 0.0 – 100.0) determines the importance to place on the fit error when calculating score and target score. An acceptance level is set for both the score and target score. A graphical line, showing the position and orientation of the marker on the drill, is constructed within the graphical cylinder using line drawing technique in computer graphics, and is displayed in real time, by using the position and orientation of the centroid of the marker and drawing the results, in the display's overlay buffer non-destructively. The line is displayed within the graphical cylinder with its axis at exact inclination as that of the axis of the pedicle canal and its dimensions exactly same as that of the pedicle canal, constructed earlier using computer graphics. The graphical results display the position and orientation of the drill and are used for real time drill control and navigation. Positional results and audio-visual alerts are used to prevent boundary violation, which can lead to pedicle wall perforation. An interactive GUI and real time video display, with real time graphical overlay is built for ease of access, for viewing position and orientation of the drill or pedicle screw during insertion.

#### D. Paired samples t-test

T-test is based on t-distribution and is considered an appropriate test for judging the significance of a sample mean or for judging the significance of difference between the means of two samples. In case two samples are related, we use paired t-test for judging the significance of the mean of difference between the two related samples. The relevant test statistic,  $t$ , is calculated from the sample data and then compared with its probable value based on t-distribution (to be read from the table that gives probable values of  $t$ , for different levels of significance for different degrees of freedom) at a specified level of significance for concerning degrees of freedom for accepting or rejecting the null hypothesis. A paired samples t-test based on a "matched-pairs sample" results from an unpaired sample that is subsequently used to form a paired sample, by using additional variables that were measured along with the variable of interest [30]. The matching is carried out by identifying pairs of values consisting of one observation from each of the two samples, where the pair is similar in terms of other measured variables. For the sample pairs  $(x_1, y_1), (x_2, y_2), \dots, (x_n, y_n)$ , we can define the difference of each pair as:  $d_i = (x_i - y_i)$ ;  $i=1, 2, 3, \dots, n$ . Under the basic assumption that the differences  $d_i$  follows normal distribution with mean value zero and fixed variance  $\sigma^2$  we define a t-statistic as follows:

$$t = \frac{\bar{d}}{S_d / \sqrt{(n-1)}}$$

Where,

$$\bar{d} = \sum_{i=1}^n \frac{d_i}{n}$$

$$S_d = \sqrt{\frac{1}{n} \sum_{i=1}^n (d_i - \bar{d})^2}$$

't' follows student 't' distribution with (n-1) degrees of freedom. We formulate the pair of hypothesis,  $H_0: \mu = 0$  Vs  $H_1: \mu \neq 0$ , for the chosen significance level ' $\alpha$ '. The best critical region is given by the condition  $|t| \geq t_{\alpha/2}$ . If the value of t lies in the C.R, it leads to the rejection of the null hypothesis [31].

### III. EXPERIMENTAL SETUP AND RESULTS

#### A. Evaluation of Real Time Object Tracking

The new technique was evaluated, by inserting the drill into the pre-determined point, of the transparent phantom model of the human vertebra, using computer assistance. Three needles were inserted into the landmark points on the phantom vertebra. The focus and zoom of the camera were adjusted so that, the three needles in the video were exactly made to coincide with the three vertical lines plotted on the reference CT image to complete the registration process. The graphical cylinder was drawn, with its axis at an inclination, exactly same as that of the pedicle canal, obtained from the reference CT image of the vertebra. The orientation of the axis of the cylinder was estimated, with respect to the three vertical lines drawn in the reference CT image of the vertebra. The online video of the drill, with the marker fixed centrally on its body was processed in sequential frames. The search of instances of marker models in the sequence of video frames was performed. The centroid of the marker model was found out in each frame of the video.

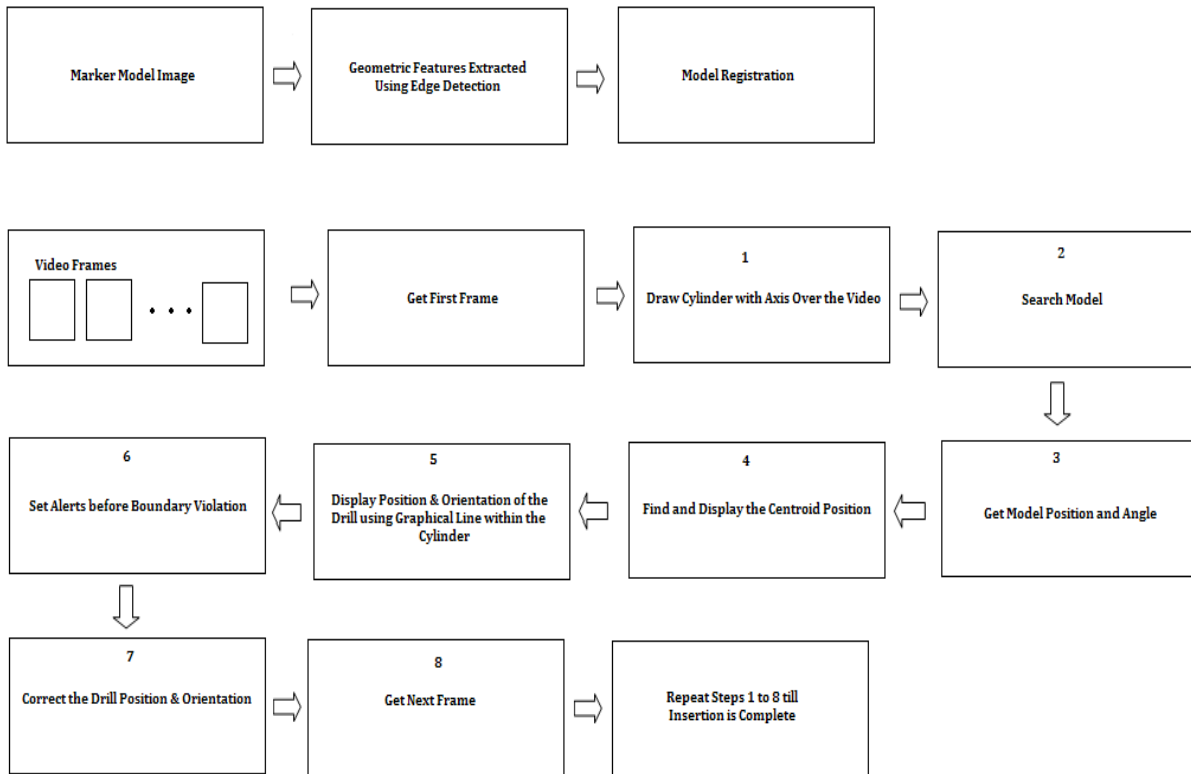


Figure4. Real time object tracking for CASS

A graphical line, showing the position and orientation of the centroid of the marker on the drill, was displayed in real time using computer graphics, and by using the position and orientation of the centroid of the marker and drawing the results, in the display's overlay buffer non-destructively[32],[33]. The drill was positioned with its burr exactly placed at the entry point on the phantom vertebra. The orientation of the drill was corrected so as to correctly enter the pedicle canal. The orientation of the drill should be the same as the marker orientation. Then, the path of the drill was tracked during insertion, so that it neither goes beyond the walls of the pedicle canal nor pierces the vertebra body. The trajectory of the burr or tip of the drill was viewed in real time, by observing the

movement of the graphical line within the cylinder. The depth of insertion was estimated by viewing the movement of the graphical line. Figure4 illustrates the procedure of real time Computer Assisted Spine Surgery (CASS). A user friendly GUI with the provision for testing camera, loading marker image, real time tracking, display positional results and search time has been developed as shown in figure 5. The centroid of the marker detected is shown in figure 6.

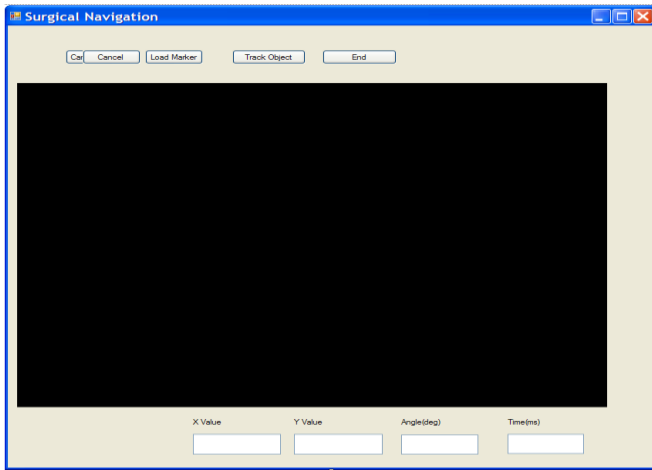


Figure5.GUI for computer assisted spine surgery



Figure6. Centroid of the marker on the micro motor drill detected

Table 2: Evaluation of Real time Computer Assisted Spine Surgery

| Real World Co-ordinates |        |        |        |                        | Image Co-ordinates |     |     |     |                   |             |               |  |
|-------------------------|--------|--------|--------|------------------------|--------------------|-----|-----|-----|-------------------|-------------|---------------|--|
| x1(cm)                  | y1(cm) | x2(cm) | y2(cm) | Real World Distance Rd | u1                 | v1  | u2  | v2  | Pixel Distance Pd | Ratio Pd/Rd | Calculated Rd |  |
| 16.4                    | 10.6   | 15     | 9.4    | 1.84                   | 422                | 429 | 406 | 441 | 20.00             | 10.85       | 1.87          |  |
| 15                      | 11.9   | 14     | 10.2   | 1.97                   | 405                | 416 | 393 | 433 | 20.81             | 10.55       | 1.95          |  |
| 12                      | 13     | 11.9   | 11.8   | 1.20                   | 368                | 406 | 372 | 418 | 12.65             | 10.50       | 1.18          |  |
| 7.7                     | 11.8   | 9      | 10.4   | 1.91                   | 311                | 424 | 327 | 437 | 20.62             | 10.79       | 1.93          |  |
| 6.8                     | 10.8   | 8.4    | 9.7    | 1.94                   | 300                | 435 | 318 | 445 | 20.59             | 10.61       | 1.93          |  |
| 7                       | 11     | 8.7    | 10     | 1.97                   | 302                | 437 | 320 | 448 | 21.10             | 10.70       | 1.98          |  |
| 11                      | 15     | 12.7   | 14     | 1.97                   | 304                | 439 | 322 | 450 | 21.10             | 10.70       | 1.98          |  |
| 10                      | 11     | 6      | 9      | 4.47                   | 275                | 463 | 321 | 450 | 47.80             | 10.69       | 4.48          |  |
| 12.7                    | 10.9   | 8.6    | 7.8    | 5.14                   | 268                | 472 | 315 | 444 | 54.71             | 10.64       | 5.12          |  |
| 13.8                    | 4.2    | 10.8   | 10.2   | 6.71                   | 255                | 481 | 318 | 446 | 72.07             | 10.74       | 6.75          |  |
| 6.9                     | 4.2    | 10.4   | 10.7   | 7.38                   | 249                | 475 | 320 | 440 | 79.16             | 10.72       | 7.41          |  |
| 5.8                     | 11.3   | 9.8    | 18.9   | 8.59                   | 233                | 462 | 322 | 443 | 91.01             | 10.60       | 8.52          |  |
| 12.7                    | 10.9   | 15.7   | 2.6    | 8.83                   | 224                | 451 | 318 | 449 | 94.02             | 10.65       | 8.80          |  |
| 9.5                     | 12.4   | 3.9    | 4.4    | 9.77                   | 217                | 446 | 321 | 445 | 104.00            | 10.65       | 9.74          |  |
| 10.9                    | 11.6   | 4.1    | 3.1    | 10.89                  | 209                | 440 | 325 | 447 | 116.21            | 10.68       | 10.88         |  |
| 10.2                    | 11.5   | 1      | 3.8    | 12.00                  | 202                | 433 | 330 | 441 | 128.25            | 10.69       | 12.01         |  |
| 14.2                    | 17.5   | 6.4    | 7      | 13.08                  | 200                | 422 | 339 | 425 | 139.03            | 10.63       | 13.02         |  |
| 11.2                    | 14.7   | 4.7    | 3.3    | 13.12                  | 191                | 370 | 331 | 375 | 140.09            | 10.68       | 13.12         |  |
| 16.5                    | 12.2   | 11.1   | 2.9    | 10.75                  | 190                | 399 | 300 | 365 | 115.13            | 10.71       | 10.78         |  |

|      |      |     |     |       |     |     |     |     |        |       |       |
|------|------|-----|-----|-------|-----|-----|-----|-----|--------|-------|-------|
| 14.1 | 11.5 | 5.6 | 1.5 | 13.12 | 160 | 385 | 299 | 365 | 140.43 | 10.70 | 13.15 |
| 14.5 | 12.7 | 6.1 | 2.5 | 13.21 | 152 | 385 | 245 | 278 | 141.77 | 10.73 | 13.27 |
| 14.8 | 12.6 | 6.8 | 3.2 | 12.34 | 134 | 363 | 245 | 292 | 131.76 | 10.67 | 12.34 |

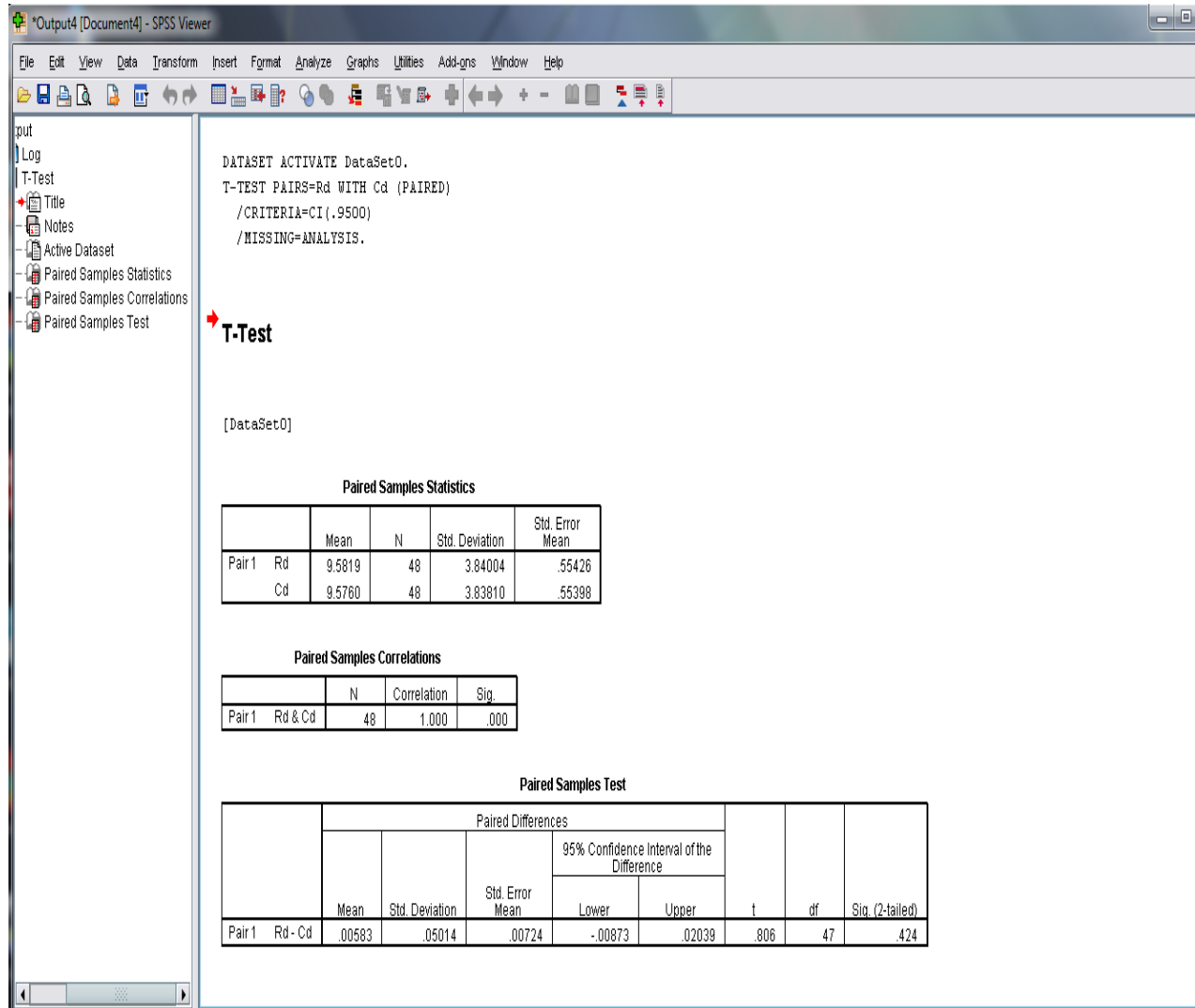


Fig 2. Output window of SPSS result viewer

**B. Evaluation of the Real Time Computer Assisted Spine Surgery**

A study on the effectiveness of the new method of tracking the drill for pedicle screw insertion was carried out comparing the real world displacement with the displacement in the image co-ordinates. The pilot hole was drilled at various positions and angles. The readings with respect to real world displacement and the corresponding displacement in the image co-ordinates have been tabulated, sample of the readings are shown in Table1. The table shows the correlation between real world displacement and displacement in the image coordinates. A comparison between them has been conducted using paired samples T test. The method is used to prove the exactness of movement of the drill using the new computer assisted navigation method. The positions of the markers on the drill were estimated using the new tracking algorithm. The (x, y) and (u, v) co-ordinate values

of the centroid for initial and final positions are tabulated both for real world and image co-ordinates. The Euclidean distances are found out using the following equations:

$$P_d = P_{d1} - P_{d2} = \sqrt{(u_1 - u_2)^2 + (v_1 - v_2)^2}$$

$$R_d = R_{d1} - R_{d2} = \sqrt{(x_1 - x_2)^2 + (y_1 - y_2)^2}$$

**C. Results**

The paired T- test procedure was performed using a sample size of 48. From each pair of observations  $(x_i, y_i)$  of  $R_d$  and  $P_d$ , the difference can be taken as  $d_i = x_i - y_i$ ;  $i=1,2,3,\dots,48$ . Set the null hypothesis  $H_0: \mu = 0$  against  $H_1: \mu \neq 0$ , where  $\mu$  denotes the mean difference. The sample values allow accepting the null hypothesis with the required level of confidence (95% confidence level). The significance level is much above 0 and its value is 0.424 as shown in fig. 2. This reveals the fact that the drill can be guided precisely and this can be stated with 95 % confidence level, which indicates good precision with a standard mean error of only 0.00724.

#### IV. CONCLUSION

A real time surgical navigation system for pedicle screw insertion was developed. The trajectory of insertion of the drill or the pedicle screw is displayed in real time and provides an aid to the surgeon, to insert the screw precisely. The system developed is cost effective and has good precision required for spine surgery.

#### REFERENCES

- [1] Caspar W, "A new microsurgical procedure for lumbar disc herniations causing less tissue damage through a microsurgical approach" *Adv Neurosurg*, 1977, 4:74-77
- [2] McCulloch JA, Young PH, *Essentials of spinal microsurgery*, Lippincott Raven, Philadelphia, 1998
- [3] Williams RW, McCulloch JA, Young PH, *Microsurgery of the lumbar spine*, Rockville, Aspen, 1990
- [4] Brau SA, "Mini-open approach to the spine for anterior lumbar interbody fusion: description of the procedure, results and complications", *Spine*, 2002, 2:216-223
- [5] Carreon LY, Puno RM, Dimar JR, et al "Perioperative complications of posterior lumbar decompression and arthrodesis in older adults", *J Bone Joint Surg*, 2003, 85A: 2089-2092
- [6] Caspar W, "A new surgical procedure for lumbar disc herniation causing less tissue damage through a microsurgical approach", *Adv Neurosurg*, 1977, 4:74-77
- [7] Tureyen K, "One-level one-sided lumbar disc surgery with and without microscopic assistance: 1-year outcome in 114 consecutive patients", *J Neurosurg*, 2003, 99:247-250
- [8] Wilson DH, Harbaugh R, "Microsurgical and standard removal of the protruded lumbar disc: a comparative Study", *J Neurosurg*, 1981, 8:422-427
- [9] Amiot LP, Labelle H, Deguise JA, Sati M, Brodeur P, Rivard CH, "Computer-assisted pedicle screw fixation A feasibility study" *Spine*, 1995, 20:1208-1212
- [10] Foley KT, Smith MM, "Image-guided spine surgery", *Neurosurg*, 1996, 7:171-186
- [11] Glossop ND, Hu RW, Randle JA, "Computer-aided pedicle screw placement using frameless stereotaxis" *Spine* 21:2026-2034
- [12] Kalfas IH, Kormos DW, Murphy MA, McKenzie RL, Barnett GH, Bell GR, Steiner CP, Trimble MB, Weisenberger JP, "Application of frameless stereotaxy to pedicle screw fixation of the spine" *J Neurosurg*, 1995, 83:641-647
- [13] Merloz P, Tonetti J, Pittet L, Coulomb M, Lavallée S, Traccaz J, Cinquin P, Sautot P "Computer assisted spine surgery" *Computer Aided Surgery*, 1998, 3:297-305
- [14] Nolte LP, Visarius H, Langlotz F, Schwarzenbach O, Berlemann U, Rohrer U, *Computer assisted spine surgery*, 1996
- [15] Amiot LP, Lang K, Putzier M, Zippel H, Labelle H "Comparative results between conventional and computer assisted pedicle screw installation in the thoracic, lumbar, and sacral spine" *Spine*, 2000, 25:606-614
- [16] Laine T, Lund T, Ylikoski M, Lohikoski J, Schlenzka D, "Accuracy of pedicle screw insertion with and without computer assistance: a randomised controlled clinical study in 100 consecutive patients" *Eur Spine J*, 2000, 9:235-240
- [17] Resnick DK, "Prospective comparison of virtual fluoroscopy to fluoroscopy and plain radiographs for placement of lumbar pedicle screws" *J Spinal Disord Tech*, 2003, 16: 254-260
- [18] Schwarzenbach O, Berlemann U, Jost B, Visarius H, ArmE, Langlotz F, Nolte LP, Ozdoba C, "Accuracy of computer- assisted pedicle screw placement, An in vivo computed tomography analysis" *Spine*, 1997, 22:452-458
- [19] Amin DV, Kanade T, Digiioia AM 3rd, Jaramaz B, Nikou C, Labarca RS, "Ultrasound-based registration of the pelvic bone surface for surgical navigation" *Comput Aided Surg*, 2001, 6:48
- [20] Foley KT, Smith MM, "Image-guided spine surgery" *Neurosurg*, 1996, 7:171-186
- [21] Fritsch E, Duchow J, Placement of pedicle screws at the entire spine with a new (Iso-C3D fluoroscopy) guidingsystem. In: Langlotz F, Davies BL, Bauer A, "Computer assisted orthopaedic surgery" Steinkopff, Darmstad, 2003, pp 106-107
- [22] Yuichi Tamura, Nobuhiko Sugano, Toshihiko Sasama, Yoshinobu Sato, Shinichi Tamura, Kazuo Yonenobu, Hideki Yoshikawa, Takahiro Ochi, "Surface-based registration accuracy of CT-based image-guided spine surgery", *Eur Spine J*, 2005, 14: 291-297
- [23] Lutz P. Nolte, M.A Slomczykowski, Uirich Berlemann, Matthias J. Strauss, Robert Hofstetter, Dietrich Schlenzka, Timo Laine, Teija Lund, "A new approach to computer aided spine surgery: fluoroscopy based surgical navigation", *Eur Spine J*, Springer-Verlag, 2000, 9 : S78-S88
- [24] Tessamma Thomas, Dinesh Kumar V.P., P.S John, Antony Joseph Thoppil, James Chacko, "A Video Based Tracking System for Pedicle Screw Fixation", *Proc. of 4th International Conference on Computer Science and its Application*, June 2006 ( ICCSA -2006 ) san Diego, California, USA
- [25] T. Ortmaier, H. Weiss, U. Hagn, M. Grebenstein, M. Nickl, A. Albu-Schäffer, C. Ott, S. J'org, R. Konietschke, Luc Le-Tien, and G. Hirzinger, "A Hands-On-Robot for Accurate Placement of Pedicle Screws", May 2006, *IEEE International Conference on Robotics and Automation*
- [26] Jon T. Lea, Dane Watkins, Aaron Mills, Michael A. Peshkin, Thomas C. Kienzle III, S. David Stulberg "Registration and immobilization in robot-assisted surgery" conference proceedings of the First International Symposium on Medical Robotics and Computer Assisted Surgery, Pittsburgh, PA, Sept.1994
- [27] Moshe Shoham, Michael Burman, Eli Zehavi, Leo Joskowicz, Eduard Batkalin, "Bone-Mounted Miniature Robot for Surgical Procedures: Concept and Clinical Applications" *IEEE Transactions On Robotics and Automation*, October 2003, VOL. 19, NO. 5
- [28] Pedram Azad, Tilo Gockel, Rüdiger Dillmann, *Computer Vision Principles and Practice 1st Edition*, Elektor International Media BV 2008
- [29] Rafael C. Gonzalez, Richard E. Woods, *Digital Image Processing*, second edition, PrenticeHall. 2004
- [30] David, HA; Gunnink, Jason L, "The Paired t Test Under Artificial Pairing". *The American Statistician*, 1997, 51 (1): 9-12
- [31] Rohatgi K. Vijay, Ehsanes Saleh Md.; 2nd Edition, *An Introduction to Probability and Statistics Wiley Series*.2010
- [32] Nobert Thomas Pallath, Tessamma Thomas, "Video Object Tracking and Analysis for Computer Assisted surgery", *The international journal of Multimedia & Its Applications (IJMA)*, February 2012, Vol.4.No.1
- [33] Nobert Thomas Pallath, Tessamma Thomas, "Real Time Computer Assisted Surgical Navigation", *IEEE International Conference on Data Science & Engineering 2012*

#### AUTHORS

**First Author** – Nobert Thomas Pallath, MSc. Electronics (CUSAT), Assoc. Professor, W.M.O Arts & Science College, Muttill, nobert.pallath@gmail.com  
**Second Author** – Dr. Tessamma Thomas, M. Tech. Digital Electronics (CUSAT) and Ph.D, Professor in the Department of

Electronics, Cochin University of Science and Technology,  
tess@cusat.ac.in

**Third Author** – Dr. S. Suresh, D(Orth),MS (Ortho),MCh (Orth),  
DNB(Orth) MNAMS Fellow (Spine Surgery), Spine Surgeon,  
Lakeshore Hospital & Research Centre, sureshorth@gmail.com